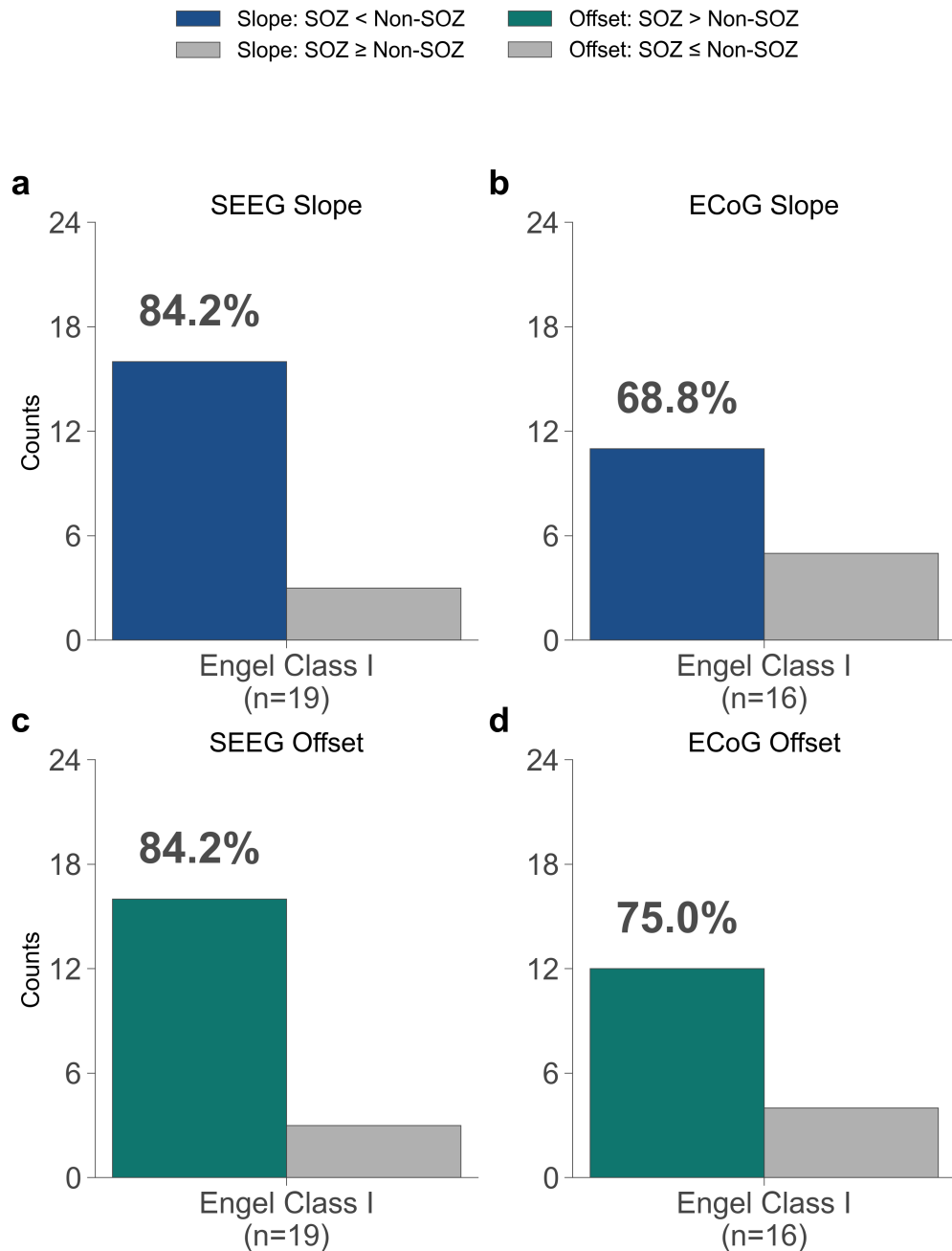


1 **Supplementary Material for ‘Interictal Scale-Free Neural Dynam-** 2 **ics Identify Epileptogenic Cortex’**

3 Marrium Shamshad, Kelley M. Smith, Kevin J. Slote, Mukesh Dhamala, and Igor
4 Belykh

5 **Supplementary Note 1: Across-patient sensitivity of interictal aperiodic abnor-** 6 **malities in Engel class I patients**

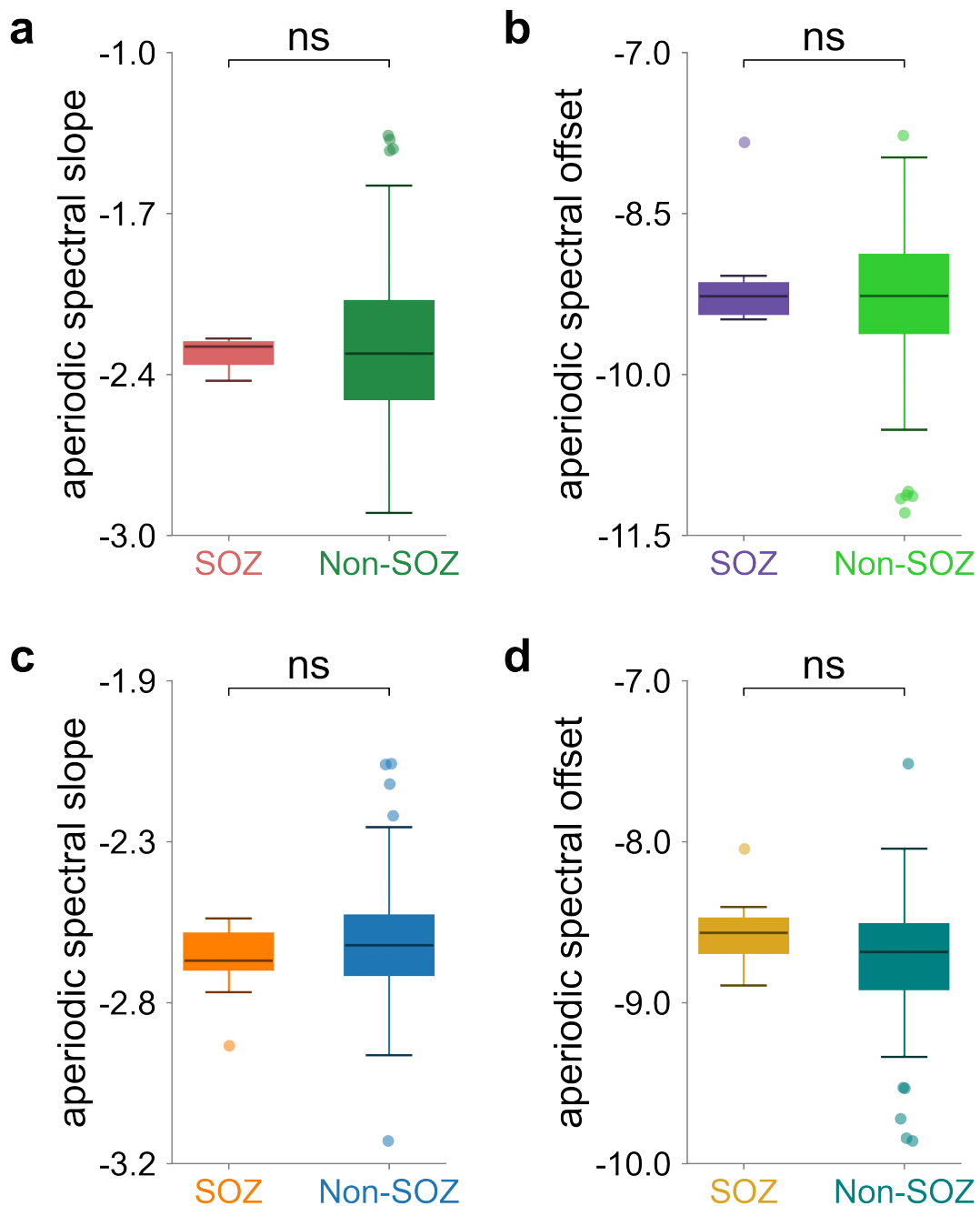
7 Supplementary Fig. 1 summarizes across-patient sensitivity of interictal SOZ aperiodic abnormalities
8 in Engel class I patients across 19 SEEG and 16 ECoG cases. Sensitivity was defined by the propor-
9 tion of patients whose SOZ–non-SOZ contrast followed the hypothesized direction, and was further
10 evaluated using group-level one-sided Wilcoxon signed-rank tests of Δ against 0, together with paired
11 Cohen’s d_z effect sizes. In SEEG, both slope and offset showed high sensitivity, with 16/19 patients
12 (84.2%) supporting the hypothesized direction for each feature, and both remained significant at the
13 group level (slope: $P = 3.918 \times 10^{-3}$, $d_z = -0.739$; offset: $P = 3.918 \times 10^{-3}$, $d_z = 0.775$). In ECoG,
14 slope was directionally consistent in 11/16 patients (68.8%) and also remained significant at the group
15 level ($P = 3.845 \times 10^{-2}$, $d_z = -0.533$), whereas offset was directionally consistent in 12/16 patients
16 (75.0%) but did not reach group-level significance ($P = 1.742 \times 10^{-1}$, $d_z = 0.281$). Overall, interictal
17 aperiodic abnormalities were more robust in SEEG than in ECoG. All reported P values are BH-FDR
18 corrected.



Supplementary Figure 1. Across-patient sensitivity of interictal SOZ aperiodic abnormalities in Engel class I patients. Patient-level SOZ–non-SOZ contrasts were classified according to whether $\Delta = \text{median}(z_{\text{SOZ}}) - \text{median}(z_{\text{non-SOZ}})$ followed the hypothesized direction. Colored bars denote patients supporting the hypothesized direction, and gray bars denote patients not supporting it; percentage labels indicate sensitivity. Group-level deviation of Δ from 0 was assessed using one-sided Wilcoxon signed-rank tests with paired Cohen’s d_z effect sizes. SEEG results were significant for slope (16/19; $P = 3.918 \times 10^{-3}$, $d_z = -0.739$) and offset (16/19; $P = 3.918 \times 10^{-3}$, $d_z = 0.775$). ECoG results were significant for slope (11/16; $P = 3.845 \times 10^{-2}$, $d_z = -0.533$) but not for offset (12/16; $P = 1.742 \times 10^{-1}$, $d_z = 0.281$). All reported P values are BH-FDR corrected.

19 **Supplementary Note 2: Representative Engel class II–IV failure cases**

20 Supplementary Fig. 2 presents representative Engel class II–IV failure cases showing weak or negli-
21 gible interictal SOZ–non-SOZ separation in aperiodic slope and offset. These SEEG and ECoG ex-
22 amples illustrate the limited and heterogeneous within-patient specificity observed in the unfavorable-
23 outcome cohort.



Supplementary Figure 2. Illustrative failure cases show weak or absent SOZ–non-SOZ separation in interictal aperiodic slope and offset. **a**, Representative SEEG failure case showing limited SOZ–non-SOZ separation in aperiodic slope (sub-HUP171; $n_{\text{SOZ}} = 3$, $n_{\text{non-SOZ}} = 145$, $P = 0.898$, $d = 0.091$, $\delta = 0.048$). **b**, Representative SEEG failure case showing similarly minimal SOZ–non-SOZ separation in aperiodic offset (sub-HUP151; $n_{\text{SOZ}} = 7$, $n_{\text{non-SOZ}} = 165$, $P = 0.785$, $d = -0.007$, $\delta = 0.063$). **c,d**, Representative ECoG failure case (sub-HUP086) showing weak SOZ–non-SOZ differentiation for slope (**c**; $n_{\text{SOZ}} = 10$, $n_{\text{non-SOZ}} = 90$, $P = 0.386$, $d = -0.266$, $\delta = -0.169$) and offset (**d**; $P = 0.222$, $d = 0.332$, $\delta = 0.269$). Together, these examples illustrate that interictal aperiodic slope and offset abnormalities were weak, variable, and not clearly separable between SOZ and non-SOZ contacts in failure cases. Here, P denotes the BH-FDR corrected two-sided Mann–Whitney test, d denotes Cohen’s d , and δ denotes Cliff’s delta.

24 **Supplementary Note 3: Within-patient SOZ–non-SOZ separability of interictal**
 25 **aperiodic slope and offset in success cases**

26 We assessed whether aperiodic slope and broadband offset separated SOZ from non-SOZ contacts
 27 within individual SEEG and ECoG success cases using one-sided Mann–Whitney U tests. Raw P
 28 values were adjusted within feature using the BH-FDR corrected procedure. Supplementary Tables 1
 29 and 2 report only patients with FDR-corrected $P < 0.05$, together with Δ , Cliff’s δ , and Cohen’s d .

30 Significant within-patient SOZ–non-SOZ separation was observed in 9/19 SEEG patients for slope
 31 and 10/19 for offset, and in 8/16 ECoG patients for slope and 7/16 for offset.

Supplementary Table 1. Patient-level within-patient SOZ–non-SOZ separability in SEEG success cases for aperiodic slope and broadband offset.

Feature	Patient ID	n_{SOZ}	$n_{\text{non-SOZ}}$	Δ median	Raw p	FDR-corrected P	Cliff’s δ	Cohen’s d
Slope	sub-HUP142	10	98	-0.454	1.514e-06	1.439e-05	-0.900	-2.115
Slope	sub-HUP141	13	100	-0.434	1.983e-07	3.767e-06	-0.868	-1.331
Slope	sub-HUP163	8	148	-0.485	4.926e-05	3.120e-04	-0.750	-1.566
Slope	sub-HUP157	6	158	-0.273	2.241e-03	6.349e-03	-0.654	-0.961
Slope	sub-HUP146	7	115	-0.185	2.339e-03	6.349e-03	-0.615	-1.009
Slope	sub-HUP134	17	66	-0.176	1.420e-03	5.745e-03	-0.472	-0.687
Slope	sub-HUP177	16	156	-0.103	1.512e-03	5.745e-03	-0.451	-0.597
Slope	sub-HUP139	11	62	-0.272	1.293e-02	3.072e-02	-0.425	-0.869
Slope	sub-HUP160	12	90	-0.097	1.772e-02	3.742e-02	-0.376	-0.709
Offset	sub-HUP141	13	100	1.245	3.994e-07	7.590e-06	0.845	1.708
Offset	sub-HUP164	3	173	0.779	3.766e-03	7.951e-03	0.823	1.302
Offset	sub-HUP157	6	158	1.140	3.111e-04	1.478e-03	0.757	1.411
Offset	sub-HUP142	10	98	0.759	7.888e-05	5.313e-04	0.729	1.398
Offset	sub-HUP163	8	148	0.863	5.045e-04	1.917e-03	0.655	1.560
Offset	sub-HUP146	7	115	0.441	2.153e-03	5.843e-03	0.620	1.100
Offset	sub-HUP134	17	66	0.617	8.390e-05	5.313e-04	0.595	1.011
Offset	sub-HUP160	12	90	0.464	1.191e-03	3.771e-03	0.543	1.112
Offset	sub-HUP177	16	156	0.394	2.582e-03	6.133e-03	0.425	0.661
Offset	sub-HUP144	15	96	0.390	9.817e-03	1.865e-02	0.376	0.564

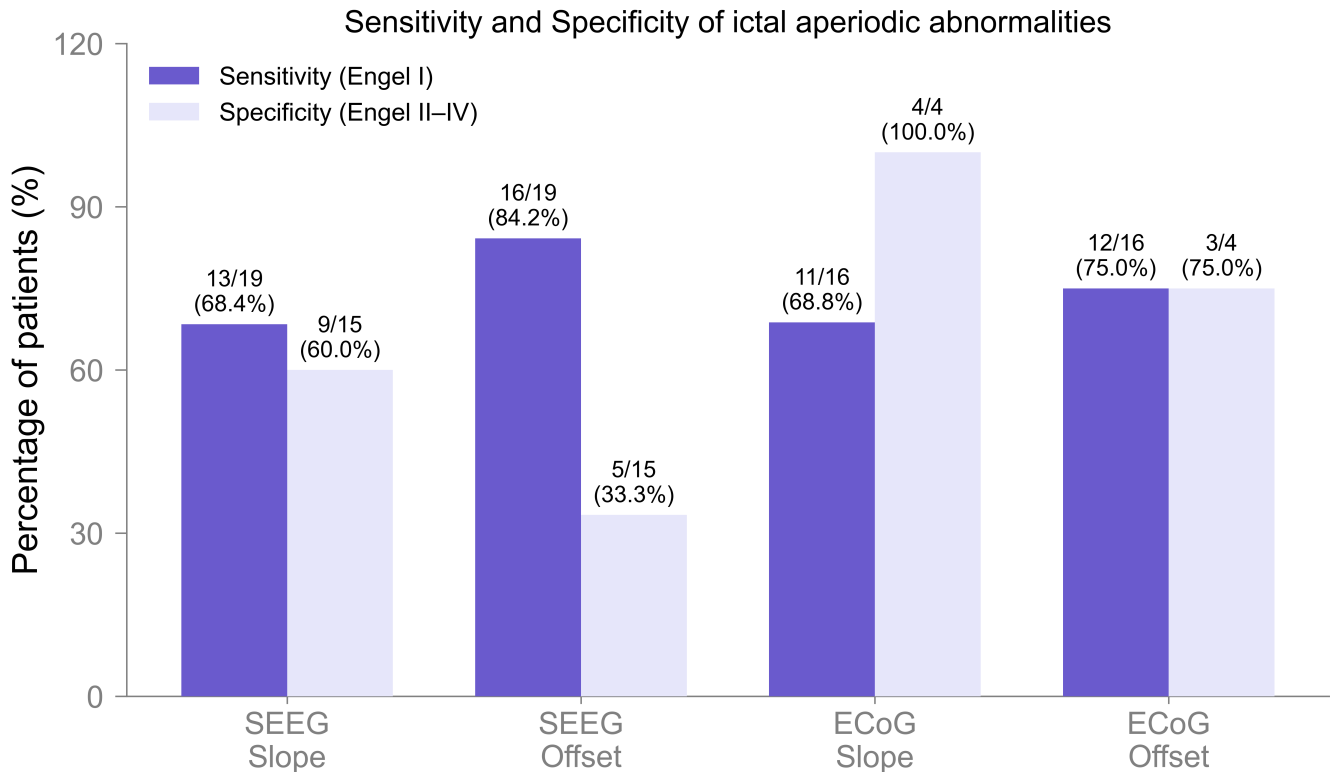
Supplementary Table 2. Patient-level within-patient SOZ–non-SOZ separability in ECoG success cases for aperiodic slope and offset.

Feature	Patient ID	n_{SOZ}	$n_{\text{non-SOZ}}$	Δ median	Raw p	FDR-corrected P	Cliff’s δ	Cohen’s d
Slope	sub-HUP126	9	116	-0.336	1.138e-05	7.637e-05	-0.851	-1.456
Slope	sub-HUP089	10	84	-0.224	6.352e-05	2.033e-04	-0.745	-1.752
Slope	sub-HUP106	10	105	-0.238	5.529e-05	2.033e-04	-0.743	-1.831
Slope	sub-HUP111	7	94	-0.317	2.155e-04	4.926e-04	-0.742	-1.378
Slope	sub-HUP065	15	49	-0.292	1.432e-05	7.637e-05	-0.720	-1.551
Slope	sub-HUP123	21	96	-0.221	1.247e-05	7.637e-05	-0.589	-1.030
Slope	sub-HUP097	15	77	-0.360	6.810e-04	1.362e-03	-0.526	-0.960
Slope	sub-HUP107	23	94	-0.135	9.409e-05	2.509e-04	-0.504	-0.812
Offset	sub-HUP089	10	84	0.529	9.618e-06	1.411e-04	0.831	1.834
Offset	sub-HUP065	15	49	1.123	1.763e-05	1.411e-04	0.712	1.624
Offset	sub-HUP106	10	105	0.376	5.181e-04	2.763e-03	0.630	1.339
Offset	sub-HUP126	9	116	0.232	1.845e-02	4.217e-02	0.420	1.057
Offset	sub-HUP123	21	96	0.480	2.773e-03	1.109e-02	0.388	0.644
Offset	sub-HUP097	15	77	0.436	1.359e-02	3.623e-02	0.363	0.607
Offset	sub-HUP107	23	94	0.157	1.089e-02	3.485e-02	0.310	0.473

Supplementary Note 4: Sensitivity and specificity of ictal aperiodic slope and offset during the first 40 s after seizure onset

To determine whether early ictal aperiodic abnormalities provide sensitive markers of epileptogenic tissue, we analyzed the first 40 s after seizure onset in Engel class I patients using patient-level SOZ–non-SOZ median contrasts. In SEEG, aperiodic slope contrasts were negative in 13/19 patients (68.4%) and remained significant at the group level ($P = 3.64 \times 10^{-2}$, $d_z = -0.485$), whereas broadband offset contrasts were positive in 16/19 patients (84.2%) and showed a stronger effect ($P = 8.39 \times 10^{-4}$, paired Cohen's $d_z = 1.108$). In ECoG, slope contrasts were negative in 11/16 patients (68.8%) and were also significant at the group level ($P = 3.64 \times 10^{-2}$, paired Cohen's $d_z = -0.571$), whereas offset contrasts were positive in 12/16 patients (75.0%) and likewise remained significant ($P = 2.50 \times 10^{-2}$, paired Cohen's $d_z = 0.513$). Overall, during the first 40 s after seizure onset, both ictal slope flattening and offset elevation remained significantly associated with the SOZ in Engel class I patients, with broadband offset showing the strongest early ictal sensitivity across modalities.

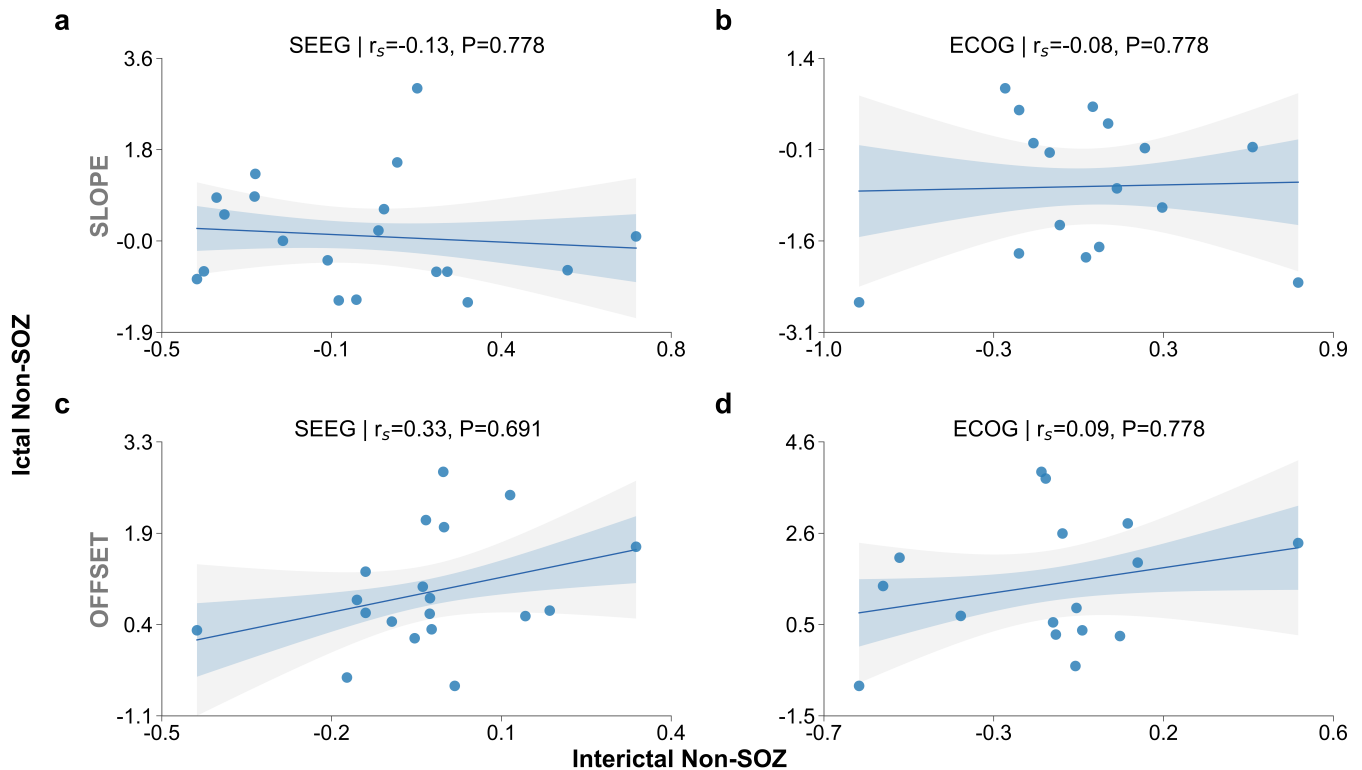
We next asked whether these early ictal abnormalities remained specifically associated with favorable outcome during the same after-onset window. In poor-outcome SEEG, specificity was modest for slope at 60.0% (9/15) and lower for offset at 33.3% (5/15). Group-level slope contrasts were not significant ($P = 4.54 \times 10^{-1}$, $d_z = -0.22$), and offset showed only a weak trend that did not survive global correction ($P = 6.03 \times 10^{-2}$, paired Cohen's $d_z = 0.71$). In poor-outcome ECoG, specificity was 100.0% (4/4) for slope and 75.0% (3/4) for offset, but neither group-level contrast was significant (slope: $P = 6.06 \times 10^{-1}$, $d_z = 0.68$; offset: $P = 6.25 \times 10^{-1}$, $d_z = 0.20$). Thus, although ictal aperiodic slope and offset during the first 40 s after seizure onset were SOZ-concordant in Engel class I patients, their outcome-consistent specificity was weaker than in the centered-onset analysis and was not supported by significant group-level effects in poor-outcome cases.



Supplementary Figure 3. Across-patient sensitivity and outcome-consistent specificity of ictal aperiodic abnormalities during the first 40 s after seizure onset. Bar plots summarize the proportion of patients whose SOZ aperiodic abnormalities followed the hypothesized direction for aperiodic slope and broadband offset in SEEG and ECoG. In Engel class I patients, after-onset sensitivity was 68.4% (13/19) for SEEG slope ($P = 3.642 \times 10^{-2}$, $d_z = -0.429$), 84.2% (16/19) for SEEG offset ($P = 8.392 \times 10^{-4}$, $d_z = 0.959$), 68.8% (11/16) for ECoG slope ($P = 3.642 \times 10^{-2}$, $d_z = -0.545$), and 75.0% (12/16) for ECoG offset ($P = 2.496 \times 10^{-2}$, $d_z = 0.668$); all four cohort-level effects remained significant after correction, with the strongest effect observed for SEEG broadband offset. In Engel class II-IV patients, outcome-consistent specificity was 60.0% (9/15) for SEEG slope ($P = 6.057 \times 10^{-1}$, paired Cohen's $d_z = -0.224$), 33.3% (5/15) for SEEG offset ($P = 6.030 \times 10^{-2}$, $d_z = 0.713$), 100.0% (4/4) for ECoG slope ($P = 6.057 \times 10^{-1}$, $d_z = 0.681$), and 75.0% (3/4) for ECoG offset ($P = 6.250 \times 10^{-1}$, $d_z = 0.205$); however, no poor-outcome cohort-level contrast remained significant after correction. These results show that early ictal slope flattening and offset elevation remained significantly enriched in the SOZ of surgically successful patients, whereas outcome-consistent specificity was weaker than in the centered-onset analysis. All reported P values are BH-FDR corrected.

56 **Supplementary Note 5: Non-SOZ cross-epoch correlations of aperiodic slope**
57 **and offset in 40 s windows**

58 We next examined whether patient-level non-SOZ aperiodic slope and offset remained stable across
59 interictal and ictal 40 s windows.



Supplementary Figure 4. Non-SOZ cross-epoch correlations of aperiodic slope and offset in 40 s windows. (a,b) Patient-level non-SOZ slope estimates computed from 40 s windows are plotted for ictal versus interictal epochs (x-axis: interictal non-SOZ; y-axis: ictal non-SOZ), shown separately for SEEG (a) and ECoG (b). (c,d) The same comparison is shown for non-SOZ offset (SEEG in c; ECoG in d). Each point denotes one patient. Spearman correlation coefficients (r_s) and corresponding P values are reported in each panel. Solid lines indicate the fitted trend, and shaded bands indicate uncertainty around the fit. Overall, non-SOZ aperiodic estimates show weak interictal–ictal coupling, consistent with non-SOZ values remaining near baseline across epochs.

60 **Supplementary Note 6: Aperiodic interictal slope and offset diagnostic metrics**
 61 **overview**

62 Supplementary Tables 3 and 4 summarize patient-level diagnostic classification performance for aperi-
 63 odic slope and offset, together with the corresponding group-level SOZ–non-SOZ contrast statistics
 64 (Wilcoxon signed-rank P -values and Cohen’s d effect sizes). These analyses were derived from the
 65 patient-level SOZ–non-SOZ contrast $D = \tilde{x}_{\text{SOZ}} - \tilde{x}_{\text{non-SOZ}}$, computed in robust z-scores. A patient was
 66 classified as test-positive when $D < 0$ for slope or $D > 0$ for offset, consistent with the SOZ pattern
 67 supported by the group-level SOZ–non-SOZ contrast statistics. Sensitivity (TPR) was defined as the
 68 fraction of Engel class I patients classified as test-positive, whereas outcome-consistent specificity
 69 (TNR) was defined as the fraction of Engel class II–IV patients classified as test-negative.

Supplementary Table 3. Patient-level diagnostic classification metrics for aperiodic slope and offset in SEEG.

Diagnostic Accuracy and Error Rate Analysis						
Feature	Accuracy	Precision (PPV)	Sensitivity (TPR)	Specificity (TNR)	False Positive Rate	False Negative Rate
Slope	60.0% (21/35)	59.3% (16/27)	84.2% (16/19)	31.2% (5/16)	68.8% (11/16)	15.8% (3/19)
Offset	62.9% (22/35)	61.5% (16/26)	84.2% (16/19)	37.5% (6/16)	62.5% (10/16)	15.8% (3/19)

Supplementary Table 4. Patient-level diagnostic classification metrics for aperiodic slope and offset in ECoG.

Diagnostic Accuracy and Error Rate Analysis						
Feature	Accuracy	Precision (PPV)	Sensitivity (TPR)	Specificity (TNR)	False Positive Rate	False Negative Rate
Slope	60.0% (12/20)	78.6% (11/14)	68.8% (11/16)	25.0% (1/4)	75.0% (3/4)	31.2% (5/16)
Offset	70.0% (14/20)	85.7% (12/14)	75.0% (12/16)	50.0% (2/4)	50.0% (2/4)	25.0% (4/16)

70 **Supplementary Note 7: High-frequency aperiodic analyses and within-patient** 71 **Mann–Whitney U statistics in Engel class I patients**

72 To further characterize within-patient SOZ abnormalities in the high-frequency range (85–155 Hz),
73 we performed node-wise Mann–Whitney U analyses comparing SOZ and non-SOZ contacts within
74 individual Engel class I patients across 30 s interictal, preictal, and ictal epochs. These analyses
75 assessed within-patient SOZ–non-SOZ separation for both high-frequency slope and high-frequency
76 offset in SEEG and ECoG. Unless otherwise noted, all reported P values denote BH-FDR corrected
77 P values.

78 **Interictal within-patient analyses**

79 During interictal epochs, significant within-patient SOZ decreases in high-frequency slope were ob-
80 served in 11/19 SEEG patients (57.9%) and 2/16 ECoG patients (12.5%), whereas significant within-
81 patient SOZ increases in high-frequency offset were observed in 8/19 SEEG patients (42.1%) and
82 2/16 ECoG patients (12.5%), respectively, at $P < 0.05$. Cohen’s d values among significant patients
83 ranged from medium to large for SEEG slope, from small to large for SEEG offset, were large for
84 ECoG slope, and ranged from medium to large for ECoG offset. As a representative SEEG case, pa-
85 tient sub-HUP164 ($n_{\text{SOZ}} = 3$, $n_{\text{non-SOZ}} = 173$) showed lower SOZ than non-SOZ high-frequency slope
86 ($P = 1.053 \times 10^{-2}$, $d = -1.871$) together with higher SOZ high-frequency offset ($P = 4.725 \times 10^{-3}$,
87 $d = 2.070$). As a representative ECoG case, patient sub-HUP065 ($n_{\text{SOZ}} = 15$, $n_{\text{non-SOZ}} = 49$) showed
88 lower SOZ high-frequency slope ($P = 1.216 \times 10^{-3}$, $d = -1.442$) and higher SOZ high-frequency
89 offset ($P = 1.141 \times 10^{-3}$, $d = 1.469$).

90 **Preictal within-patient analyses**

91 During preictal epochs, significant within-patient SOZ decreases in high-frequency slope were ob-
92 served in 7/19 SEEG patients (36.8%) and 6/16 ECoG patients (37.5%), whereas significant within-
93 patient SOZ increases in high-frequency offset were observed in 7/19 SEEG patients (36.8%) and
94 5/16 ECoG patients (31.2%), respectively, at $P < 0.05$. Cohen’s d values among significant patients
95 ranged from small to large for SEEG slope, from medium to large for SEEG offset, and were uniformly

96 large for both slope and offset in ECoG. As a representative SEEG case, patient sub-HUP164 showed
97 lower SOZ than non-SOZ high-frequency slope ($P = 1.489 \times 10^{-4}$, $d = -2.495$) together with higher
98 SOZ high-frequency offset ($P = 1.489 \times 10^{-4}$, $d = 2.810$). As a representative ECoG case, patient
99 sub-HUP094 ($n_{\text{SOZ}} = 3$, $n_{\text{non-SOZ}} = 80$) showed lower SOZ high-frequency slope ($P = 1.350 \times 10^{-3}$,
100 $d = -1.453$) and higher SOZ high-frequency offset ($P = 6.060 \times 10^{-3}$, $d = 1.232$).

101 **Ictal within-patient analyses**

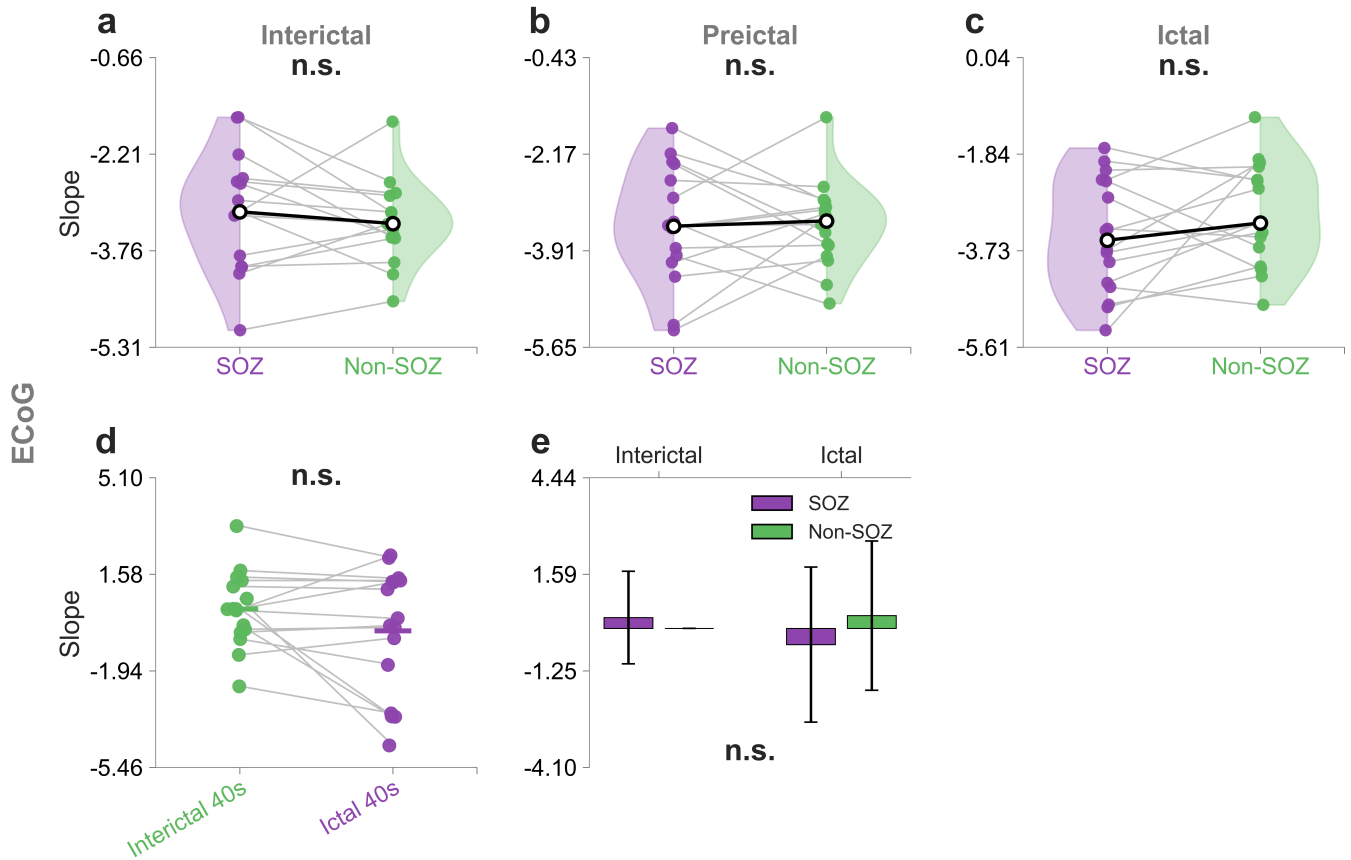
102 During ictal epochs, significant within-patient SOZ decreases in high-frequency slope were observed
103 in 10/19 SEEG patients (52.6%) and 7/16 ECoG patients (43.8%), whereas significant within-patient
104 SOZ increases in high-frequency offset were observed in 12/19 SEEG patients (63.2%) and 8/16
105 ECoG patients (50.0%), respectively, at $P < 0.05$. Cohen's d values among significant patients
106 ranged from medium to large for both SEEG features, whereas all significant ECoG effects were
107 large for both slope and offset. As a representative SEEG case, patient sub-HUP164 showed lower
108 SOZ than non-SOZ high-frequency slope ($P = 4.963 \times 10^{-5}$, $d = -2.792$) together with higher SOZ
109 high-frequency offset ($P = 1.418 \times 10^{-5}$, $d = 3.112$). As a representative ECoG case, patient sub-
110 HUP065 showed lower SOZ high-frequency slope ($P = 2.325 \times 10^{-7}$, $d = -2.703$) and higher SOZ
111 high-frequency offset ($P = 2.229 \times 10^{-7}$, $d = 2.770$).

112 Overall, these within-patient Mann–Whitney U analyses indicate that high-frequency aperiodic
113 SOZ abnormalities were detectable across interictal, preictal, and ictal states in both modalities, with
114 the strongest and most consistent within-patient separation generally observed during ictal epochs.

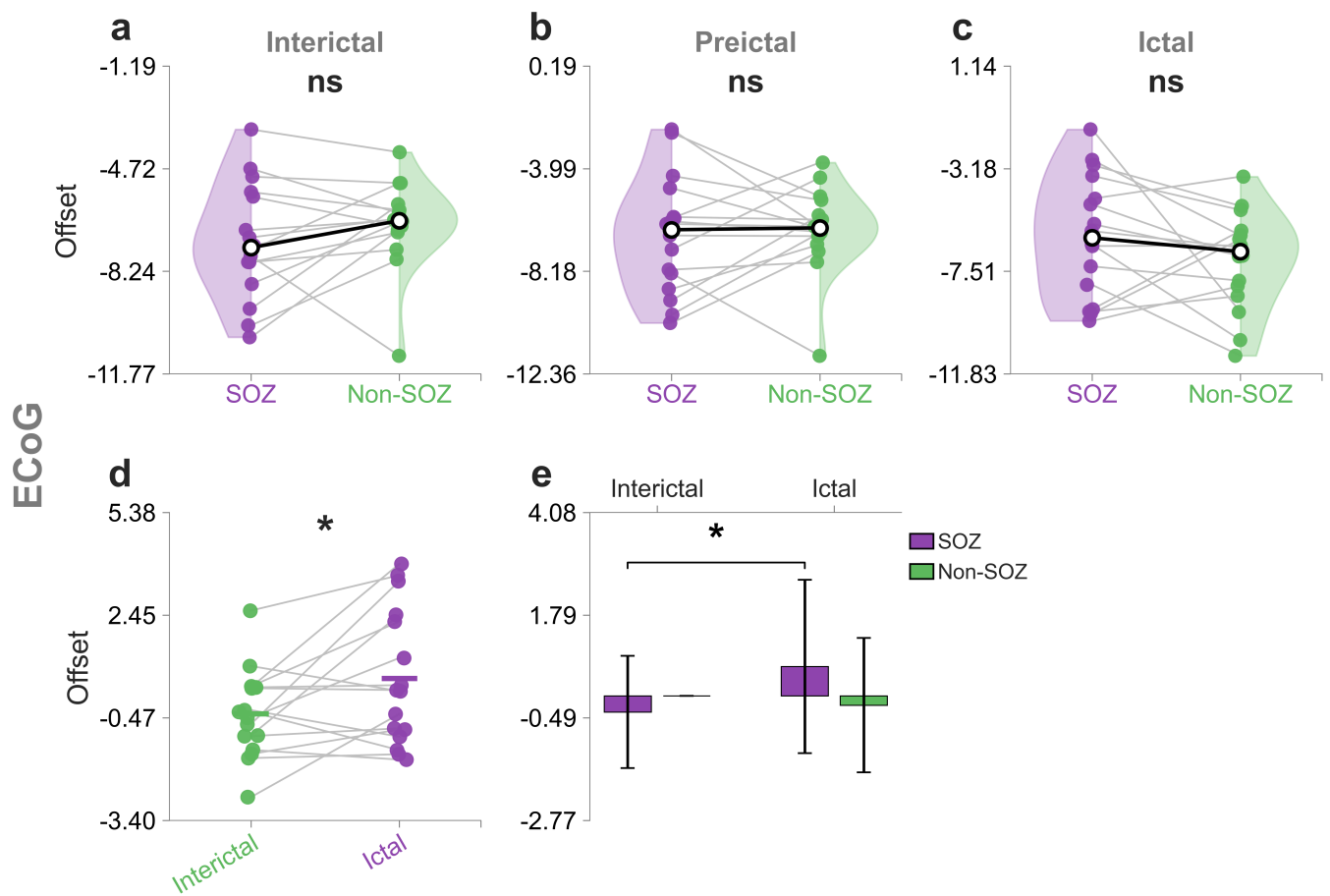
115 **High-frequency ECoG aperiodic abnormalities are weaker and less consistent**
116 **across states**

117 In ECoG Engel class I patients ($N = 16$), high-frequency slope and offset abnormalities were weaker
118 and less consistent than in SEEG, and no within-epoch comparison remained significant after epoch-
119 wise FDR-correction. During interictal epochs, slope and offset followed the hypothesized directions in
120 only 6/16 patients (37.5%), and the group-level median contrasts were opposite to the hypothesized
121 SOZ-supporting pattern (slope: median $\Delta_{\text{slope}} = 0.313$, IQR $[-0.457, 1.189]$, $P = 8.943 \times 10^{-1}$;
122 offset: median $\Delta_{\text{offset}} = -0.385$, IQR $[-1.094, 0.394]$, $P = 8.943 \times 10^{-1}$). Results remained non-
123 significant during the preictal period, where shifts were observed in 9/16 patients (56.2%; slope:
124 median $\Delta_{\text{slope}} = -0.043$, IQR $[-1.316, 1.545]$, $P = 5.500 \times 10^{-1}$; offset: median $\Delta_{\text{offset}} = 0.029$, IQR
125 $[-1.658, 1.175]$, $P = 5.500 \times 10^{-1}$). During the ictal state, directional consistency increased modestly
126 to 10/16 patients (62.5%), but neither feature reached significance after correction (slope: median
127 $\Delta_{\text{slope}} = -0.728$, IQR $[-2.235, 0.562]$, BH-FDR $P = 7.953 \times 10^{-2}$; offset: median $\Delta_{\text{offset}} = 0.485$, IQR
128 $[-0.455, 2.284]$, BH-FDR $P = 7.778 \times 10^{-2}$).

129 Between epochs, paired within-SOZ interictal-to-ictal slope changes in ECoG did not reach sig-
130 nificance (one-sided Wilcoxon signed-rank test; $N = 16$; Supplementary Fig. 5d). By contrast, SOZ
131 offset increased modestly from interictal to ictal states (one-sided Wilcoxon signed-rank test; interictal
132 $<$ ictal; $N = 16$; $p = 0.0288$; Supplementary Fig. 6d). Together, these findings indicate that high-
133 frequency aperiodic abnormalities in ECoG were weaker and less consistent across patients than
134 those observed in SEEG.



Supplementary Figure 5. ECoG aperiodic slope (high frequency). a–c, SOZ versus non-SOZ patient-level paired medians across interictal, preictal and ictal epochs. d,e, SOZ interictal versus ictal comparisons in 30 s windows. Across panels, slope effects did not reach significance ($N = 16$).



Supplementary Figure 6. ECoG aperiodic offset (high frequency). **a–c**, SOZ versus non-SOZ patient-level paired medians across interictal, preictal and ictal epochs. **d,e**, SOZ offset increased from interictal to ictal in 30 s windows ($p = 0.0288$; $N = 16$).

136 **Supplementary Note 8: High-frequency specificity and diagnostic performance**
137 **in Engel class II–IV patients**

138 **Within-patient high-frequency specificity**

139 We next assessed whether high-frequency (85–155 Hz) aperiodic slope avoided false positive re-
140 inforcement of the clinically labeled SOZ in patients with unsuccessful surgical outcomes (Engel
141 classes II–IV). Specificity (true negative rate, TNR) was defined as the fraction of Engel class II–
142 IV patients who were not test-positive in the hypothesized SOZ direction. A patient was considered
143 test-positive only if the within-patient SOZ–nonSOZ contrast was in the hypothesized direction and
144 remained significant after BH-FDR correction of the corresponding one-sided within-patient Mann–
145 Whitney U test. Using this criterion, slope showed moderate specificity across epochs in the pooled
146 cohort ($N = 20$): 60.0% (interictal; 12/20), 70.0% (preictal; 14/20), and 50.0% (ictal; 10/20).

147 Stratified by modality, SEEG ($N = 16$) specificity was 50.0% (interictal; 8/16), 62.5% (preictal;
148 10/16), and 37.5% (ictal; 6/16), whereas ECoG ($N = 4$) showed 100% specificity in all epochs (4/4
149 each), although interpretation of ECoG specificity is limited by the small failure cohort.

150 Representative true-negative examples included interictal SEEG sub-HUP166 ($n_{\text{SOZ}} = 15, n_{\text{non-SOZ}} =$
151 149, $P = 1.261 \times 10^{-2}$, $\delta = 0.496$, $d = 0.848$), preictal SEEG sub-HUP166 ($P = 7.814 \times 10^{-3}$), ictal
152 SEEG sub-HUP166 ($P = 3.848 \times 10^{-3}$), interictal ECoG sub-HUP086 ($P = 2.711 \times 10^{-6}$), preictal
153 ECoG sub-HUP086 ($P = 5.920 \times 10^{-5}$), and ictal ECoG sub-HUP086 ($P = 5.735 \times 10^{-3}$).

154 **Across-epoch offset specificity**

155 Using the same specificity criterion, 85–155 Hz aperiodic offset showed similar specificity across
156 epochs. In the pooled cohort ($N = 20$), specificity was 65.0% (interictal; 13/20), 70.0% (preictal;
157 14/20), and 50.0% (ictal; 10/20).

158 In SEEG ($N = 16$), specificity was 50.0% (interictal; 8/16), 62.5% (preictal; 10/16), and 37.5%
159 (ictal; 6/16), while ECoG ($N = 4$) again showed 100% specificity in all epochs, with the same caveat
160 regarding small sample size.

161 Representative true-negative examples included interictal SEEG sub-HUP166 ($P = 5.174 \times 10^{-3}$),

162 preictal SEEG sub-HUP166 ($P = 3.931 \times 10^{-3}$), ictal SEEG sub-HUP166 ($P = 6.471 \times 10^{-4}$), and
163 interictal ECoG sub-HUP086 ($P = 3.825 \times 10^{-6}$).

164 **Patient-level within-epoch summary statistics**

165 Supplementary Table 5 summarizes patient-level within-epoch high-frequency slope and offset analy-
 166 ses in the 85–155 Hz range for SEEG and ECoG in the Engel class I cohort. Within each epoch, one
 167 patient-level SOZ–nonSOZ contrast was computed per patient as $D = \tilde{x}_{\text{SOZ}} - \tilde{x}_{\text{nonSOZ}}$. Group-level
 168 significance was then assessed across patients using one-sided Wilcoxon signed-rank tests against
 169 $D = 0$, followed by BH-FDR correction within each epoch across the four tests (SEEG slope, SEEG
 170 offset, ECoG slope, ECoG offset). For slope, the hypothesized SOZ-supporting direction was $D < 0$,
 171 whereas for offset it was $D > 0$. Significant within-epoch effects were observed in SEEG across
 172 interictal, preictal, and ictal epochs for both slope and offset after epoch-wise false-discovery-rate
 173 correction, whereas no ECoG comparison survived correction.

Supplementary Table 5. Patient-level within-epoch high-frequency aperiodic summary statistics for SEEG and ECoG in Engel class I patients. Within each epoch, one patient-level SOZ–nonSOZ contrast was computed per patient in the 85–155 Hz range. The table reports the number of patients in the hypothesized direction (Direction n), percentage, median contrast (Δ), interquartile range (IQR), Wilcoxon signed-rank statistic, raw p -value, and BH-FDR corrected P -value.

Modality	Feature	Epoch	N	Direction	n	%	Median Δ	IQR	W	Raw p	BH-FDR P
SEEG	Slope	Interictal	19	15	78.9	-0.628	[-0.740, -0.225]	21.0	8.469×10^{-4}	2.399×10^{-3}	
SEEG	Slope	Preictal	19	12	63.2	-0.597	[-0.892, 0.147]	37.0	9.041×10^{-3}	1.808×10^{-2}	
SEEG	Slope	Ictal	19	17	89.5	-0.721	[-1.591, -0.214]	19.0	5.856×10^{-4}	1.171×10^{-3}	
SEEG	Offset	Interictal	19	15	78.9	0.609	[0.229, 0.802]	167.0	1.200×10^{-3}	2.399×10^{-3}	
SEEG	Offset	Preictal	19	13	68.4	0.597	[-0.077, 0.858]	153.0	9.041×10^{-3}	1.808×10^{-2}	
SEEG	Offset	Ictal	19	17	89.5	1.103	[0.417, 1.296]	179.0	1.049×10^{-4}	4.196×10^{-4}	
ECoG	Slope	Interictal	16	6	37.5	0.313	[-0.457, 1.189]	85.0	8.123×10^{-1}	8.943×10^{-1}	
ECoG	Slope	Preictal	16	9	56.2	-0.043	[-1.316, 1.545]	69.0	5.301×10^{-1}	5.500×10^{-1}	
ECoG	Slope	Ictal	16	10	62.5	-0.728	[-2.235, 0.562]	40.0	7.953×10^{-2}	7.953×10^{-2}	
ECoG	Offset	Interictal	16	6	37.5	-0.385	[-1.094, 0.394]	44.0	8.943×10^{-1}	8.943×10^{-1}	
ECoG	Offset	Preictal	16	9	56.2	0.029	[-1.658, 1.175]	66.0	5.500×10^{-1}	5.500×10^{-1}	
ECoG	Offset	Ictal	16	10	62.5	0.485	[-0.455, 2.284]	99.0	5.833×10^{-2}	7.778×10^{-2}	

Supplementary Table 6. Across-patient directional diagnostic performance of high-frequency (85–155 Hz) aperiodic slope and offset across interictal, preictal, and ictal 30 s epochs in SEEG.

Epoch	Feature	Accuracy	Precision (PPV)	Sensitivity (TPR)	Specificity (TNR)	False Positive Rate	False Negative Rate
Interictal	Slope	67.6% (23/34)	68.2% (15/22)	78.9% (15/19)	53.3% (8/15)	46.7% (7/15)	21.1% (4/19)
Interictal	Offset	67.6% (23/34)	68.2% (15/22)	78.9% (15/19)	53.3% (8/15)	46.7% (7/15)	21.1% (4/19)
Preictal	Slope	61.8% (21/34)	66.7% (12/18)	63.2% (12/19)	60.0% (9/15)	40.0% (6/15)	36.8% (7/19)
Preictal	Offset	64.7% (22/34)	68.4% (13/19)	68.4% (13/19)	60.0% (9/15)	40.0% (6/15)	31.6% (6/19)
Ictal	Slope	61.8% (21/34)	60.7% (17/28)	89.5% (17/19)	26.7% (4/15)	73.3% (11/15)	10.5% (2/19)
Ictal	Offset	61.8% (21/34)	60.7% (17/28)	89.5% (17/19)	26.7% (4/15)	73.3% (11/15)	10.5% (2/19)

Supplementary Table 7. Across-patient directional diagnostic performance of high-frequency (85–155 Hz) aperiodic slope and offset across interictal, preictal, and ictal 30 s epochs in ECoG.

Epoch	Feature	Accuracy	Precision (PPV)	Sensitivity (TPR)	Specificity (TNR)	False Positive Rate	False Negative Rate
Interictal	Slope	50.0% (10/20)	100.0% (6/6)	37.5% (6/16)	100.0% (4/4)	0.0% (0/4)	62.5% (10/16)
Interictal	Offset	50.0% (10/20)	100.0% (6/6)	37.5% (6/16)	100.0% (4/4)	0.0% (0/4)	62.5% (10/16)
Preictal	Slope	65.0% (13/20)	100.0% (9/9)	56.2% (9/16)	100.0% (4/4)	0.0% (0/4)	43.8% (7/16)
Preictal	Offset	65.0% (13/20)	100.0% (9/9)	56.2% (9/16)	100.0% (4/4)	0.0% (0/4)	43.8% (7/16)
Ictal	Slope	70.0% (14/20)	100.0% (10/10)	62.5% (10/16)	100.0% (4/4)	0.0% (0/4)	37.5% (6/16)
Ictal	Offset	70.0% (14/20)	100.0% (10/10)	62.5% (10/16)	100.0% (4/4)	0.0% (0/4)	37.5% (6/16)

Supplementary Table 8: Overview of patient demographics in Dataset.

Patient ID	Dataset ID	Gender	Age at Surgery	Engel Score
sub-HUP064	sub-HUP064	M	21	1D
sub-HUP065	sub-HUP065	M	36	1B
sub-HUP070	sub-HUP070	M	33	1B
sub-HUP074	sub-HUP074	F	25	1C
sub-HUP082	sub-HUP082	F	56	1A
sub-HUP087	sub-HUP087	M	24	1D
sub-HUP088	sub-HUP088	F	35	1D
sub-HUP089	sub-HUP089	M	29	1B
sub-HUP094	sub-HUP094	F	48	1B
sub-HUP097	sub-HUP097	F	39	1D
sub-HUP105	sub-HUP105	M	39	1A
sub-HUP106	sub-HUP106	F	45	1B
sub-HUP107	sub-HUP107	M	36	1A
sub-HUP111	sub-HUP111	F	40	1B
sub-HUP116	sub-HUP116	F	59	1A
sub-HUP117	sub-HUP117	M	39	1A
sub-HUP123	sub-HUP123	M	36	1A
sub-HUP126	sub-HUP126	F	26	1A
sub-HUP130	sub-HUP130	F	46	1B
sub-HUP134	sub-HUP134	M	32	1B
sub-HUP139	sub-HUP139	M	20	1A
sub-HUP140	sub-HUP140	F	47	1B
sub-HUP141	sub-HUP141	M	30	1C
sub-HUP142	sub-HUP142	M	30	1D
sub-HUP144	sub-HUP144	M	31	1D
sub-HUP146	sub-HUP146	M	16	1A
sub-HUP148	sub-HUP148	M	23	1A
sub-HUP150	sub-HUP150	M	17	1B
sub-HUP157	sub-HUP157	M	25	1B
sub-HUP160	sub-HUP160	F	45	1A
sub-HUP163	sub-HUP163	F	42	1D
sub-HUP164	sub-HUP164	F	34	1D
sub-HUP177	sub-HUP177	F	42	1A
sub-HUP180	sub-HUP180	F	28	1A
sub-HUP185	sub-HUP185	M	38	1A
sub-HUP080	sub-HUP080	F	41	2C
sub-HUP086	sub-HUP086	F	25	2A
sub-HUP135	sub-HUP135	M	37	2A
sub-HUP151	sub-HUP151	M	33	2A
sub-HUP171	sub-HUP171	M	50	2A
sub-HUP172	sub-HUP172	F	28	2A

Patient ID	Dataset ID	Gender	Age at Surgery	Engel Score
sub-HUP187	sub-HUP187	M	25	2A
sub-HUP060	sub-HUP060	F	42	3A
sub-HUP112	sub-HUP112	F	21	3A
sub-HUP114	sub-HUP114	F	43	3A
sub-HUP133	sub-HUP133	F	52	3A
sub-HUP162	sub-HUP162	F	35	3A
sub-HUP165	sub-HUP165	F	21	3A
sub-HUP166	sub-HUP166	M	26	3A
sub-HUP179	sub-HUP179	F	20	3A
sub-HUP181	sub-HUP181	F	31	3A
sub-HUP188	sub-HUP188	F	24	3A
sub-HUP190	sub-HUP190	M	25	3A
sub-HUP075	sub-HUP075	F	57	4A
sub-HUP138	sub-HUP138	M	38	4A

Supplementary Table 8. Patient demographics of the included HUP cohort. All data was collected from the Hospital of the University of Pennsylvania (HUP).